N71-20532

NASA CR-72834

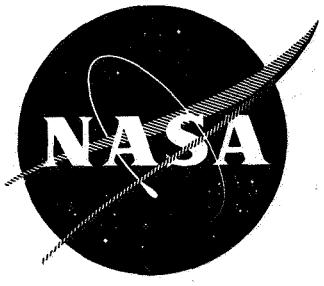

CASE FILE COPY

1970 ANNUAL REPORT ON THE INVESTIGATION OF CRITICAL PRESSURE BURNING OF FUEL DROPLETS

by

G. M. Faeth
Mechanical Engineering Department
The Pennsylvania State University
University Park, Pennsylvania

prepared for

National Aeronautics and Space Administration

January 1971

Contract NGR 39-009-077

Technical Management
NASA Lewis Research Center
Cleveland, Ohio
Dr. R. J. Priem

NOTICE

This report was prepared as an account of Government sponsored work. Neither the United States, nor the National Aeronautics and Space Administration (NASA), nor any person acting on behalf of NASA:

A.) Makes any warranty or representation, expressed or implied, with respect to the accuracy, completeness, or usefulness of the information contained in this report, or that the use of any information, apparatus, method, or process disclosed in this report may not infringe privately owned rights; or

B.) Assumes any liabilities with respect to the use of, or for damages resulting from the use of any information, apparatus, method or process disclosed in this report.

As used above, "person acting on behalf of NASA" includes any employee or contractor of NASA, or employee of such contractor, to the extent that such employee or contractor of NASA, or employee of such contractor prepares, disseminates, or provides access to, any information pursuant to his employment or contract with NASA, or his employment with such contractor.

Requests for copies of this report should be referred to

National Aeronautics and Space Administration
Scientific and Technical Information Facility
P. O. Box 33
College Park, MD 20740

NASA CR-72834

1970 ANNUAL REPORT ON THE INVESTIGATION OF CRITICAL PRESSURE BURNING OF FUEL DROPLETS

by

G. M. Faeth

Mechanical Engineering Department
The Pennsylvania State University
University Park, Pennsylvania

prepared for

National Aeronautics and Space Administration

January 1971

Contract: NGR 39-009-077

Technical Management
NASA Lewis Research Center
Cleveland, Ohio

Dr. R. J. Priem

Foreword

This annual report on NASA contract NGR 39-009-077 covers the period January 1, 1970 through December 31, 1970. This research is concerned with the combustion characteristics of liquid propellants at high pressures, with particular emphasis on conditions where the liquid approaches its critical point. The study was under the direction of G. M. Faeth, Associate Professor of Mechanical Engineering.

Contributors to this report include:

C. Allison, Ph.D. Candidate - Section III

G. S. Canada, Ph.D. Applicant - Section IV

R. S. Lazar, Ph.D. - Section II

Dr. Lazar has left the university following the completion of his doctoral dissertation on the project. The active participation of these people is gratefully acknowledged.

Table of Contents

Table of Contents (Continued)

1970 ANNUAL REPORT ON THE INVESTIGATION OF CRITICAL PRESSURE BURNING OF FUEL DROPLETS

Summary

This report discusses activities under NASA Contract NGR 39-009-077 for the period January 1, 1970 through December 31, 1970. The work was divided into four phases, the results under each phase may be summarized as follows:

1. High Pressure Droplet Combustion. These experiments considered the combustion of n-octane and n-decane droplets in air under zero-gravity conditions. A low pressure model and a high pressure model (which allowed for dissolved gases) were developed for comparison with the experiments. It was found that dissolved gases in the liquid phase significantly influence droplet conditions at high pressures. For combustion in air, the products may be taken to be equivalent to nitrogen in determining solubility characteristics due to the predominance of nitrogen in the system. The calculations were found to be most sensitive to a parameter proportional to the Lewis number. Thus the convenient unity Lewis number assumption should not be made, unless strictly valid, if accurate predictions of droplet conditions at high pressures are to be obtained.

2. Atmospheric Pressure Flat Flame Study. The burning rates of 1200μ diameter droplets of hydrazine, MMH and UDMH were measured in the combustion products of a flat flame burner. The tests were conducted at atmospheric pressure with gas temperatures of 1650-2550 K and oxygen concentrations in the range 0-42% by mass. The burning rates of the three fuels were similar, exhibiting a slow increase with increasing ambient temperature and a rapid increase with increasing ambient oxygen concentration. At comparable ambient oxygen concentrations, the present burning rates are 30-50% higher than results obtained at room temperatures. Tests are continuing with porous spheres to obtain data for a range of droplet sizes prior to analyzing the data.

3. High Pressure Flat Flame Study. A high pressure flat flame burner apparatus was designed and its construction is nearing completion. This apparatus will be employed to determine burning rates and droplet conditions at high pressures in a combustion gas environment. The droplets will be simulated using the porous sphere technique.

4. Liquid Strand Combustion. An apparatus was constructed to allow measurements of the liquid phase temperature distribution of burning monopropellant strands. The tests considered ethyl nitrate, normal propyl nitrate, and propylene glycol dinitrate at pressures up to 85 atmospheres. Comparison of theoretical

and experimental liquid surface temperatures supports the need for considering dissolved gas effects at high pressures. The calculations were found to be most sensitive to a parameter proportional to the Lewis number. The calculations were less sensitive to variations in solubility parameters, which is fortunate since these are well known for only a few propellants. The requirement for sensible heating of the liquid phase results in a substantial increase in the pressure required for supercritical combustion when compared with steady droplet burning with the droplet uniformly at its wet bulb temperature. This suggests that supercritical droplet burning criteria based on steady burning models underestimate the pressure required for supercritical combustion -- except for the later stages of burning where internal temperature gradients have relaxed.

I. Introduction

The objective of this investigation is to study the combustion and evaporation of liquid fuels at high pressures. Particular emphasis is placed on conditions where the liquid surface approaches its thermodynamic critical point during combustion. This report gives a summary of progress on the investigation for the period January 1, 1970 to December 31, 1970.

Work during this report period was divided into four phases: (1) High Pressure Droplet Combustion, involving the analysis of steady droplet burning under zero gravity conditions. (2) Atmospheric Pressure Flat Flame Study, where measurements were made of droplet burning rates in a combustion gas environment for hydrazine, MMH and UDMH. (3) High Pressure Flat Flame Study, involving the development of a pressurized flat flame burner system for studying droplet burning in a combustion gas environment. (4) Liquid Strand Combustion, which considers the analysis of high pressure effects on the equilibrium surface state of a burning liquid monopropellant column.

In the following sections the work in each phase is summarized for the report period. Wherever possible, the details of the work are presented by reference to past publications and only material not previously reported is given extended coverage.

II. High Pressure Droplet Combustion

Introduction:

This portion of the investigation considered steady droplet combustion at high pressures. The experimental apparatus for this work consisted of a high pressure chamber within which droplets were ignited and burned under zero gravity conditions. Difficulties were encountered in obtaining experimental droplet burning rates at high pressures. Therefore, the work primarily emphasized the state of the droplet during steady burning and the pressures required for the onset of supercritical burning, since measurements of this type could be obtained to test the theoretical predictions.

The findings of this portion of the investigation are presented in some detail in Refs. 1-3. These results are briefly summarized in the following, with emphasis on activities during this report period.

Baseline Tests:

In order to provide a baseline for the analysis of high pressure combustion, burning rate measurements were made with droplets subjected to the combustion products of a flat flame burner. These measurements were previously compared with a constant average property burning rate model in NASA CR-72622 (Ref. 4). Further consideration of the problem

indicated that it would be desirable to re-calculate these results using a variable property solution. In this way, arbitrary fitting of the results is not possible through judicious selection of average properties, providing a more basic test of the theory.

The variable property solution employed for this analysis was first presented by Goldsmith and Penner.[5] This model was chosen since it postulates property variations that are particularly suitable for the fuels considered in the present study. Use of the standard heat of reaction for the energy release in the droplet flame was found to yield absurdly high flame temperatures. Therefore, a partial allowance was made for dissociation in the flame by computing the chemical energy release as a function of temperature, allowing for all relevant dissociation reactions. The burning rate was then determined by trial and error until the computed flame temperature agreed with the temperature used to evaluate the heat release.

Results with the variable property model were similar to the constant property results given in Ref. 4 (for the constant property solution, properties were evaluated at the log mean temperature and average composition, with dissociation corrections applied at the flame.) Absolute differences between the two models were less then 15%. After considering various sources of theoretical and experimental error, the conclusions remain the same as those given in Ref. 4. The theory continues to systematically overestimate the burning rate of the heavier hydrocarbons. This failure with respect to increasing fuel molecular weight is felt to be due to fuel decomposition in the gas phase near the droplet surface.

Experimental Apparatus:

Work on high pressure droplet combustion was conducted with a zero-gravity apparatus in order to prevent the droplet from falling due to reduced surface tension near the critical point. Test droplets were supported from a fine wire (.002 in. O.D.) thermocouple junction and ignited within a small pressurized chamber.

Measurements were made of the steady droplet burning temperature as a function of pressure. The pressures required for supercritical combustion were also measured (the onset of this condition was determined by the continuous rise of droplet temperature following ignition, with no inflection to indicate an approach to a steady burning state). Burning rates were also determined at low pressures, however, optical difficulties due to flame luminousity and refraction prevented similar measurements at high pressures. The experiments considered n-decane and n-octane droplets burning in air.

Theoretical Analysis:

Workers at the University of Wisconsin have shown that dissolved gas in the liquid phase is an important factor in determining droplet conditions at high pressures.[6,7] Thus, for the analysis of the high pressure data, the Goldsmith and Penner[5] theory was extended to allow for the evaporation of dissolved gas along with the fuel. The analysis

was also extended to allow the computation of the composition of fuel, oxidizer and all product and inert species in the gas phase.

Two basic models were employed to evaluate phase equilibrium at the drop surface. In the first model high pressure effects were neglected. The fuel mole fraction at the droplet surface was calculated as the ratio of the vapor pressure of the fuel, at the droplet temperature, to the total pressure. Similarly, the heat of vaporization of the fuel was evaluated at the droplet temperature and dissolved gases were neglected. This model is reasonably accurate at low pressures and has also been used by Wieber[8] for estimating supercritical burning conditions.

The second model considered high pressure corrections and ambient gas solubility. Droplet phase equilibrium was determined by equality of pressure, temperature, and the fugacity of each component in both gas and liquid phases. The fugacities were determined from the Redlich-Kwong equation of state with mixing rules suggested by Prausnitz and Chueh.[9] The binary interaction parameters required in the mixing rules of the Redlich-Kwong equation of state were obtained for systems of n-paraffin hydrocarbons in nitrogen, carbon dioxide,and water by fitting the equation to available binary phase equilibrium data.

Two versions of the high pressure model were considered. The first treated the complete quaternary system fuel, nitrogen, and the combustion products, carbon dioxide and water. Due to the predominance of nitrogen in the system for combustion in air, the second model assumed that the combustion products were equivalent to nitrogen and only the binary system fuel-nitrogen was considered.

Results:

For n-decane droplets, the experimental supercritical combustion condition was reached at pressures between 650 and 700 psia (P_r=2.13 to 2.30, where P_r is the reduced pressure with respect to the critical pressure of the pure fuel). For n-octane droplets the supercritical burning condition was found between 850 and 900 psia (P_r=2.35 to 2.49).

The two versions of the high pressure theory gave essentially the same results and were in reasonable agreement with the data both with respect to steady burning temperatures and the pressures required for the onset of supercritical combustion. The low pressure model underestimated the pressure required for supercritical combustion by roughly a factor of two. The sensitivity of the calculated results to errors in properties was examined by parametrically varying the binary interaction parameters, the combustion temperature, and the transport quantity $\chi = \lambda/(CD)$ where λ is the thermal conductivity, C the molar concentration, and D the binary diffusivity. The most critical parameter was found to be χ. The results of the determination of supercritical burning conditions are summarized in Table I (the limits on the computed results are due to $\pm$ 20% variations in χ).

Summary and Conclusions:

The results indicate that ambient gas solubility and high pressure corrections should be considered in determining droplet conditions at high pressures for the heavier paraffin hydrocarbons. For combustion in air, these phase equilibrium calculations can be simplified by taking the properties of the combustion products equivalent to nitrogen. Uncertainties in the calculations are primarily introduced by uncertainties in the transport parameter χ. Since this parameter is proportional to the Lewis number, arbitrarily setting the Lewis number equal to unity (to simplify the calculations) can lead to large errors for heavier hydrocarbons.

The calculations indicate that the pressure required for supercritical combustion approaches the critical pressure of the pure fuel as the molecular weight decreases for the paraffin hydrocarbons.

The burning rate results indicate that the presently used droplet combustion models progressively overestimate the burning rate with increasing fuel molecular weight. It is suggested that fuel decomposition between the droplet surface and the oxidation zone be examined as a possible cause for this failure.

III. Atmospheric Pressure Flat Flame Study

Introduction:

This portion of the investigation considers droplet burning in the combustion products of a flat flame burner. The work during the past year extended an earlier study of fuel droplet combustion,[4] to the hydrazine fuels. The propellants specifically considered in the investigation included hydrazine, mono-methylhydrazine (MMH), unsymmetrical dimethyl hydrazine (UDMH) and Aerozine 50. The experimental testing was conducted at atmospheric pressure.

A number of previous investigations have considered droplet combustion for the hydrazine fuels.[10-15] For the most part, these earlier studies employed ambient gases around the droplet at temperatures near room temperature. One exception to this is the study by Kosvic and Breen,[15] which also considered hydrazine droplet combustion in high temperature combustion products. However, the range of the tests of Ref. (15) is somewhat limited. Thus the present investigation will provide more extensive experimental results at conditions represenative of combustion chamber conditions.

Since the hydrazine fuels exhibit exothermic decomposition, combustion in an oxidizer often involves a decomposition region followed by an oxidation zone. Therefore, these systems involve some of the characteristics of both monopropellants and bipropellants. This complicates theoretical modeling of droplet burning rates. Thus another objective of the study was to provide a more extensive test of the two flame theory of hydrazine combustion proposed by Beltran, et al,[13] than has been possible in the past.

Experimental Apparatus:

The flat flame burner apparatus has been described in detail in Ref. 4. Briefly, the apparatus consists of a burner mounted on rails so that it can be rapidly moved under the test droplet to begin the combustion process. The burner was operated with mixtures of carbon monoxide, hydrogen, oxygen, and nitrogen to yield various oxygen concentrations and temperatures at the droplet location.

The temperature and composition of the burned gas flowing around the droplet was determined from thermochemical calculations allowing for all relevant dissociation reactions and heat loss to the burner. The thermochemical properties for these calculations were taken from the JANAF Tables.[16] The gas velocity at the droplet location was calculated from the measured mass flux into the burner and the known properties of the burned gas. Table II summarizes the computed properties of the gas for all test conditions.

Droplet burning rates were measured employing both the suspended droplet and porous sphere techniques. For the suspended droplet method, the droplet was supported from a quartz fiber having a diameter of approximately 100μ. The time variation of droplet diameter was measured from motion picture shadowgraphs as described in Ref. 4.

Figure 1 shows a sample plot of diameter squared as a function of time for three tests with UDMH. Since this type of plot was reasonably linear, the data was summarized by measuring the slop of these curves to yield burning rate constants. The slopes were determined by fitting a least squares curve to the data for each test. The slope was balanced about a fixed average diameter (on the order of 1200μ) in order to reduce variations from the diameter squared law, valid for motionless evaporating droplets, due to convection and decomposition effects.[4] At each test condition, the reported burning rate constant is the average of three separate tests.

Figure 2 shows a sketch of the porous sphere system. It was necessary to cool the fuel feed line to prevent excessive fuel preheating from the hot burner gases. The fuel was forced through the sphere with a calibrated syringe pump. The steady burning condition was fixed by the fuel flow rate that would keep the sphere wet without dripping.

Eastman Organic fuels were employed in the testing; hydrazine (95+% purity), MMH (boiling point 87-88C), and UDMH (boiling point 61-63C). Aerozine 50 (A-50) was blended in this laboratory from these materials. In addition, some tests were conducted with analyzed UDMH (99.8% purity) supplied by the FMC Corporation.

Results:

The results to be presented were obtained with the supported droplet technique. The porous sphere testing and the analysis of the data is not complete at this time and will be presented at a later date.

The effect of the diameter of the quartz fiber on the results was investigated in preliminary testing. It was found that doubling the diameter of the fiber from 100 to 200μ resulted in a 15% increase in burning rate. This suggests that the present results may be somewhat in excess of the burning rates of free droplets.

Figure 3 illustrates the influence of ambient temperature on the burning rate at conditions with negligible ambient oxygen concentration. The burning rates of the three fuels are quite similar and there is little difference in behavior between the two UDMH samples. As the temperature increases from 1660 to 2470 K, the burning rate increases roughly 50%. The bulk of the increase occurs at temperatures greater than 2200 K, particularly for MMH and UDMH.

The influence of ambient oxygen concentration at a fixed ambient temperature of 2530 K is shown in Figure 4. The increase in burning rate with oxygen concentration is similar for the three fuels, amounting to a 100% increase as the oxygen mass fraction goes from .043 to .418. The higher purity UDMH appears to have a consistantly higher burning rate than the standard sample, with maximum differences of about 20%.

For burning in room temperature air, Dykema and Greene[11] measured burning rates of .016 and .011 cm^2/sec for hydrazine and UDMH with droplet sizes similar to those used in the present tests. The comparable values from the present experiments (at the same oxygen concentration) are .021 for hydrazine and .0145 (std), .0168 (99.8% purity) for UDMH. Thus the higher ambient temperature of the present tests yields a 30-50% increase in burning rate at this oxygen concentration although other factors may contribute as well since there were differences in convection and the composition of the other components of the gas.

Similar suspended droplet tests were attempted with Aerozine 50. Results were not obtained, however, due to droplet shattering during burning. A further attempt will be made to test this fuel with the porous sphere technique.

For the results presented in Figures 3 and 4 the ambient gas was completely dry. Therefore, some tests were conducted to determine the influence of water vapor in the ambient gas. The results of these tests are summarized in Table III. In general, the presence of water vapor caused a slight reduction in the burning rate (which could also have been due to reduced flow velocities). The influence of the ambient composition of the gas will be investigated in greater detail using the porous sphere system.

Summary and Conclusions:

The burning rates of hydrazine, MMH, and UDMH are similar and exhibit a strong increase with increasing ambient oxygen concentrations even at the high ambient temperatures of the present tests. At comparable ambient oxygen concentrations, the present burning rates are 30-50% higher than earlier tests at room temperature.

At the present time testing is in progress using the porous sphere technique. Following these tests, the experimental results will be analyzed with particular attention given to the two flame theory of Beltran et al.[13]

IV. High-Pressure Flat Flame Study

Introduction:

Since the zero-gravity apparatus did not yield data on droplet burning rates at high pressures, a pressurized flat flame burner rig is under development to supply this information. This apparatus has the additional advantage of providing a realistic simulation of the gas environment of a burning droplet in a high pressure combustion chamber.

The high pressure flat flame burner is similar to the apparatus employed for atmospheric pressure testing, with the exception that only porous sphere testing is planned for this system. This technique has the advantage of eliminating transient effects (which become troublesome at high pressures), substantially simplifying interpretation of the data. The porous sphere also allows accurate positioning of thermocouples in the liquid phase. Work to date has been limited to the design and construction of the apparatus.

Experimental Apparatus:

Critical combustion conditions for a porous sphere experiment differ from those of a droplet. This is due to the fact that the flame must also supply a liquid phase enthalpy rise (from the initial temperature to the surface temperature) in the case of the porous sphere, in addition to the heat of vaporization required in a droplet experiment. Therefore, the first step in designing the high pressure flat flame experiment consisted of determining the pressures required for supercritical combustion.

Supercritical burning conditions for the porous sphere were computed for n-pentane, n-decane, n-hexadecane, in the absence of convection. The analysis of Refs. 1 and 3 was employed for these calculations. For the porous sphere, the net flux of dissolved gas is zero inside the reaction zone since only fuel is entering the system. Initial liquid temperatures of 75, 150, and 300 F were considered in the calculations as well as a $\pm$ 20% parametric variation of the liquid phase enthalpy change. The calculated pressures required for critical burning, allowing for real gas effects are given in Table IV.

These results indicate that the lighter hydrocarbons require lower pressures for supercritical combustion; particularly if the liquid is preheated. Since convection should reduce the pressures required for critical burning, it appears that critical burning can be observed at pressures on the order of 1500 psia. Naturally real gas effects become important at pressures below this.

A schematic diagram of the high pressure flat flame apparatus is shown in Figure 5. The apparatus consists of a high pressure reactor, fitted with windows to allow observation of the combustion process. The gas flows are metered to the burner through critical flow orifices. The burned gas exhausts through a cooler, water trap and reactor pressure control valve. The fuel is fed to the porous sphere with a variable speed diaphragm pump; with the fuel flow rate being metered at the inlet of the pump.

The reactor is designed for a working pressure of 1500 psia. It has an internal volume of 5 inches ID by 18 inches long. The inside walls are insulated with alumina fire-brick. The pressure release assembly consists of a rupture disk set at 2000 psia. In order to achieve high flow stability, the burner gases are metered with critical flow orifices. The design of these units is similar to that described by Anderson and Friedman.[17] The orifices are constructed from jewels with 10 orifices in the size range .003-.018 inch I.D. to provide flexibility in varying flow rates. The ten orifices are mounted in a single brass bar for each assembly. The orifices have been calibrated for CO, H_2, O_2, and N_2 using a wet test meter.

The flat flame burner is illustrated in greater detail in Figure 6. The burner is constructed of stainless steel and brass. The mixing chamber is filled with steel wool and fine wire gauze. A layer of copper shot is used to conduct heat from the base of the sintered bronze plate to the copper cooling coil.

An annular flow of nitrogen diluent is provided around the flat flame. This flow helps to stabilize the shape of the flame as well as assisting in the cooling of the system for high pressure operation.

The hot gases leaving the reactor enter a heat exchanger where they are cooled and finally exhausted to the atmosphere through a control valve. The heat exchanger has 0-ring seals at the cool end that allow for expansion of the components without the development of excessive stresses. The water trap at the downstream end of the heat exchanger is designed to collect water condensed from the combustion gases to prevent clogging of the micro-regulating pressure control valve.

The assembly of this apparatus is now nearly completed and it is expected that preliminary testing will begin in a short time.

V. Liquid Strand Combustion

Introduction:

The purpose of this portion of the study is to investigate temperature and dissolved gas concentrations in an evaporating column of liquid heated from the gas phase. The experimental procedure has employed burning liquid monopropellant strands. The use of this system simplifies analysis since the flow is one dimensional and steady. With

this technique it is also relatively easy to obtain results at high pressures where solubility effects become important.

The work described in this report considers only steady combustion. Some of these results have already been presented in Ref. 2. In the future, the influence of finite pressure oscillations on the combustion process will also be considered.

Experimental Apparatus:

A sketch of the experimental apparatus is given in Figure 7. The general experimental procedure is similar to that employed in Refs. 18-20. The monopropellant is placed in a glass tube contained within a windowed chamber. After pressurizing the chamber with nitrogen to the desired test pressure, the propellant is ignited with a heater coil. Following ignition, the liquid burns down the tube, allowing the combustion zone to sweep across the thermocouple. The rate of regression of the liquid column as well as the position of the thermocouple in the liquid phase is determined from motion picture shadowgraphs taken through the windows of the chamber. The test data consists of a complete liquid phase temperature record as well as the burning rate of the propellant.

The pressure vessel used in the present experiments has an inside diameter of 2 1/2 inches with an inside length of 11 inches. The chamber is rated to 6000 psia. The windows have a 1 inch diameter viewing space. The liquid column is back lighted with an arc lamp and photographed with a motion picture camera operating at speeds on the order of 30 frames per second.

Propellant tubes of various sizes have been used in the test program, however, the bulk of the data was obtained with a 4 mm I. D. tube. Liquid temperatures were obtained with .0003 inch O.D. platinum-platinum 10% rhodium butt welded thermocouples. These thermocouples were constructed following the procedures described in Ref. 21. The thermocouples are stretched horizontally through holes burned in the glass tube and sealed in place with wax. The horizontal configuration minimizes the conduction error of the thermocouple. The thermocouple output is recorded on an oscillograph with flat frequency response to 2000 cps.

Theoretical Analysis:

Due to the steady nature of this combustion process, the gas and liquid phases may be considered separately. These two results are then patched together by appropriate phase equilibria analysis at the liquid surface.

The gas phase is complicated by the decomposition process of the fuel. However, two limiting cases may be studied which substantially simplify the analysis. The two limits are: (1) infinite activation energy assumption, where the reaction zone is infinitely thin compared to the distance between the reaction zone and the liquid surface and (2) zero activation energy assumption where the reaction rate is taken

to be independent of temperature. Work to date has been confined to case (1) the infinite activation energy assumption since it represents a more realistic model for the fuels considered in this study. In this case, the solution for the gas phase to determine surface conditions is essentially the same as Refs. 1 and 3, with the exception that the oxidation zone is absent.

The combustion product composition and the flame temperature are computed from equilibrium thermochemical calculations allowing for all relevant dissociation reactions. Three fuels have been considered thus far, normal propyl nitrate (NPN), ethyl nitrate (EN), and propylene glycol dinitrate (PGDN). The flame zone properties resulting from the calculations for these fuels are given in Table V. This table lists only the major components that were considered in the analysis. The influence of pressure on flame properties is small so that the properties given in Table V have been used throughout the pressure range of the present investigation.

Two models were taken for phase equilibrium at the liquid surface. The first was a simplified model neglecting high pressure corrections and ambient gas solubility. The second, more complete, model allows for high pressure effects and the solubility of the combustion products in the liquid phase. For the three fuels, there was not sufficient phase equilibrium data in the literature to obtain the fuel-product binary interaction parameters required by the high pressure theory. Therefore, these parameters were estimated using the hydrocarbon homomorphs of the three fuels.

Results:

Although not a major objective of this study, the data was reduced to yield strand burning rates (the rate of regression of the liquid surface down the tube). These results are given in Table VI for EN, NPN, and PGDN.

The present EN burning rates are about 3% higher than Steinberger's[18] measurements and 10% higher than the values reported by Hildenbrand and Whittaker.[19] The present measurements for NPN are in good agreement with Amster, et al[22] over the limited range available for comparison (50-70 atm). Measurements of PGDN strand burning rates could not be found in the literature for comparison with the present results.

The variation of the experimental and theoretical liquid surface temperatures of EN with pressure are plotted in Fig. 8. The boiling point curve of the pure fuel is also shown on the figure for comparison.

At higher pressures, an unstable or turbulent combustion region was encountered.[19] Temperature measurements could not be made in this region, giving rise to the upper bound of experimental data in Fig. 8. The present measurements are in poor agreement at the higher pressures with earlier EN measurements by Hildenbrand and Whittaker.[19] The cause for this discrepancy is not known at the present time.

The low and high pressure theories are shown as bands rather than single curves in Fig. 8. The bands give the limits resulting from parametric variation of $\pm$ 20% on combustion temperature, $\pm$ 20% on χ_f (λ/CD_f where λ is the thermal conductivity, C the molar concentration and D_f the binary diffusivity of the fuel) and binary interaction parameters ranging from zero up to the values for the hydrocarbon homomorph of the propellant. The upper ends of the curves for the low pressure theory are terminated at conditions where the interface becomes critical (this occurs at pressures higher than those plotted in Figure 8 for the high pressure theory).

The liquid surface temperatures are well below the boiling temperature at elevated pressures and the critical condition is not reached until the pressure is substantially greater than the critical pressure of the pure fuel. For EN, the low pressure theory overestimates the surface temperature, while the high pressure theory is in good agreement with the present data.

Similar surface temperature results are given for NPN and PGDN in Figs. 9 and 10. The high pressure theory is again quite adequate for NPN, while the agreement is poorer for PGDN. The larger number of components in the PGDN system as well as the large concentration of water in the system could be contributing factors towards the increased error in this case (water is difficult to model in the phase equilibria calculations since it is polar).

Figure 11 shows a plot of the gas and liquid phase compositions at the interface as a function of pressure for EN. The critical mixing point is indicated by the equality of liquid and gas phase compositions at this condition. At high pressures, dissolved gas concentrations become quite large, reaching 35% for EN at the critical burning state.

The computed total pressures for critical combustion are given in Table VII. The ranges on these figures result from a $\pm$ 20% variation of χ_f. The low pressure theory predicts critical combustion at pressures 40-50% lower than those given by the high pressure theory. In general, the pressure required for critical strand combustion is higher than the pressure required for critical steady droplet combustion for the same fuel. This is due to the continuing requirement for sensibly heating the fuel from its initial temperature to the surface temperature in the case of strand combustion.

Summary and Conclusions:

The present results support the findings of the earlier droplet burning work in regard to the need for considering ambient gas solubility at high pressures. While binary interaction constants are not well known for these monopropellants, the calculations are not particularly sensitive to these parameters and the values for the hydrocarbon homomorphs appear to be adequate. As in the case of bipropellant droplet combustion, the calculations were most sensitive to variations in the transport parameter, χ_f.

The requirement for sensible heating of the liquid phase results in substantially increasing the pressure required for supercritical combustion. This suggests that supercritical droplet burning criteria based on steady combustion models (as in Refs. 1 and 3) may be conservative and really only apply to the later stages of droplet burning.

The present experimental technique is limited to monopropellants, but readily yields results on surface conditions at high pressures. The upper pressure limit is largely fixed by the onset of turbulent combustion; but fortunately this limit is sufficiently high for the method to yield interesting results on high pressure effects. Work is continuing in this apparatus with the hyrazine fuels; hydrazine, MMH, and UDMH.

References

1. Lazar, R. S. and Faeth, G. M., "Bipropellant Droplet Combustion in the Vicinity of the Critical Point," 13th Symposium (International) on Combustion, Salt Lake City, Utah, August, 1970.

2. Lazar, R. S. and Faeth, G. M., "Gas Solubility Effects During High Pressure Liquid Propellant Combustion," Seventh JANAF Liquid Propellant Combustion Instability Meeting, Jet Propulsion Laboratory, Pasadena, California, October, 1970.

3. Lazar, R. S., "Bipropellant Droplet Combustion in the Vicinity of the Critical Point," Ph.D. Thesis, The Pennsylvania State University, September, 1970.

4. Faeth, G. M. and Lazar, R. S., "Bipropellant Droplet Burning Rates and Lifetimes in a Combustion Gas Environment," NASA CR-72622, December, 1969.

5. Goldsmith, M. and Penner, S. S., "On the Burning of Single Drops of Fuel in an Oxidizing Atmosphere," Jet Propulsion, Vol. 24, No. 4, 1954, pp. 245-251.

6. Manrique, J. A., "Theory of Droplet Vaporization in the Region of the Thermodynamic Critical Point", NASA CR-72574, 1969.

7. Savery, W. and Borman, G. L., "Experiments on Droplet Vaporization at Supercritical Pressures", AIAA Paper No. 70-6, January, 1970.

8. Wieber, P. R., "Calculated Temperature Histories of Vaporizing Droplets to the Critical Point", AIAA Journal, Vol. 1, No. 12, November, 1963, pp. 2764-2770.

9. Prausnitz, J. M. and Chueh, P. L., Computer Calculations for High Pressure Vapor-Liquid Equilibria, p. 18, Prentice-Hall, 1968.

10. Rosser, W. A. Jr., "The Decomposition Burning of Monopropellant Drops: Hydrazine, Nitromethane, and Ethyl Nitrate," Progress Report No. 20-305, Jet Propulsion Laboratory, Pasadena, California, January 1957.

11. Dykema, O. W. and Greene, S. A., "An Experimental Study of RP-1, UDMH, and N_2H_4 Single Droplet Burning in Air and Oxygen," Liquid Rockets and Propellants, Progress in Astronautics and Rocketry, Vol. 2, Academic Press, New York, 1960, pp. 299-324.

12. Lawver, B. R., "Some Observations on the Combustion of N_2H_4 Droplets," AIAA Paper No. 65-355, AIAA Second Annual Meeting, San Francisco, California, July, 1965.

13. Beltran, M.R., et al, "Analysis of Liquid Rocket Engine Combustion Instability", Air Force Rocket Propulsion Laboratory, Technical Report No. AFRPL-TR-65-254, January, 1966.

14. del Notario, P. P. and Tarifa, C. S., "An Experimental Investigation on the Combustion of Monopropellant Droplets," AFOSR TN 59-628 January, 1959.

15. Kosvic, T. C. and Breen, B. P., "Study of Additive Effects on Hydrazine Combustion and Combustion Stability at High Pressure", AFRPL-TR-69-12, November, 1969.

16. Jones, W. H. (Chairman), JANAF Thermochemical Tables, Dow Chemical Company, Midland, Michigan.

17. Anderson, J. W. and Friedman, R., "An Accurate Metering System for Laminar Flow Studies," The Review of Scientific Instruments, Vol. 20, January, 1949, p. 66.

18. Steinberger, R., "Mechanism of Burning of Nitrate Esters", Fifth Symposium (International) on Combustion, Reinhold, New York, 1955, pp. 205-211.

19. Hildenbrand, D. L., Whittaker, A. G., and Euston, C. B., "Burning Rate Studies I. Measurement of the Temperature Distribution in Burning Liquid Strands", J. Phys. Chem., Vol. 58, 1954, pp. 1130-1133.

20. Whittaker, A. G., et al, "Burning Rate Studies. Part 7. Onset of Turbulent Combustion of Liquids Contained in Small Tubes", J. Phys. Chem., Vol. 62, 1958, pp. 908-12.

21. Fristrom, R. M. and Westenberg,A. A., Flame Structure, McGraw-Hill Book Company, New York, 1965, pp. 170-174.

22. Amster, A. B., Edwards, G. D., and Levy, J. B., "Research on the Safety Characteristics of Normal Propyl Nitrate II. Terminal Report," NAVORD Report 4493, U. S. Naval Ordnance Laboratory, Silver Spring, Maryland, March, 1957.

TABLE I

Measured and Predicted Pressures Required for Supercritical Combustion in Air

Fuel	n-Pentane	n-Octane	n-Decane
Measured Critical P_r	- - - -	2.35-2.49	2.13-2.30
Predicted Critical P_r (low pressure theory)	1.08-1.26	1.18-1.43	1.23-1.50
Predicted Critical P_r (high pressure theory)[a]	1.20-1.70	1.65-2.25	1.75-2.75

[a]Results for complete quaternary system and combustion products taken equivalent to nitrogen essentially the same.

TABLE II

PROPERTIES OF THE AMBIENT GAS FOR VARIOUS TEST CONDITIONS

Y_x	T_∞ (°K)	V_∞ (cm/sec)	PRODUCT MOLE FRACTION							
			CO	CO_2	NO	N_2	O	O_2	H_2	H_2O
.043	2530	53.4	.098	.478	.008	.370	.003	.043	0	0
.132	2530	53.4	.050	.436	.014	.358	.006	.137	0	0
.233	2530	53.4	.038	.450	.015	.237	.008	.252	0	0
.328	2530	53.4	.031	.446	.014	.136	.010	.362	0	0
.418	2530	53.4	.027	.440	.009	.042	.011	.471	0	0
0	2470	55.7	.291	.421	0	.284	0	0	0	0
0	2330	55.7	.251	.373	0	.374	0	0	0	0
0	2255	55.7	.223	.333	0	.444	0	0	0	0
0	2165	55.7	.200	.300	0	.500	0	0	0	0
0	2060	55.7	.182	.273	0	.545	0	0	0	0
0	1935	55.7	.429	.286	0	.286	0	0	0	0
0	1835	55.7	.375	.250	0	.375	0	0	0	0
0	1750	55.7	.333	.222	0	.444	0	0	0	0
0	1660	55.7	.300	.200	0	.500	0	0	0	0
0	1835	43.2	.315	.375	0	.138	0	0	.030	.142
0	1750	43.2	.283	.342	0	.219	0	0	.029	.127
0	1660	43.2	.250	.306	0	.306	0	0	.028	.111

TABLE III

INFLUENCE OF WATER VAPOR ON HYDRAZINE BURNING RATES

Temperature °K	Mole Fraction of H_2O in Burned Gas	% Reduction in Burning Rate from Value With No H_2O
1835	.142	8.1
1750	.127	8.2
1660	.111	4.6

TABLE IV

PRESSURE REQUIRED FOR CRITICAL BURNING

POROUS SPHERE COMBUSTION (psia)

Initial Temperature (°F)	n-pentane	n-decane	n-hexadecane
300	855	1520	1650
150	1000	1750	1750
75	---	1825	1850
75 (+20%)	---	1975	2060
75 (-20%)	---	1670	1850

TABLE V

ASSUMED COMBUSTION ZONE PROPERTIES

Fuel	Flame Temperature (°K)	COMBUSTION PRODUCT MOLE FRACTIONS				
		N_2	H_2	CO	CO_2	H_2O
NPN	1350	.090	.470	.440	0	0
EN	1900	.100	.355	.375	0	.170
PGDN	3000	.144	.118	.319	.116	.303

TABLE VI

STRAND BURNING RATES

Pressure (Atm)	BURNING RATE (cm/sec)		
	EN	NPN	PGDN
20.4	.208	--	.231
30.6	.309	--	.363
40.8	.389	--	.482
51.0	.436	.153	.608
61.2	.482	.188	--
71.4	--	.221	--
81.6	--	.227	--
92.0	--	.246	--

TABLE VII

CALCULATED CRITICAL BURNING PRESSURES†

	EN	NPN	PGDN
Critical Pressure (atm)	48.3	41.1	35.4
Critical Burning Pressure Low Pressure Theory (atm)	74-92	78-100	70-92
Critical Burning Pressure High Pressure Theory (atm)	104-140	136-190	103-154
Critical Burning P_r Low Pressure Theory	1.53-.189	1.91-2.43	1.98-2.58
Critical Burning P_r High Pressure Theory	2.15-290	3.31-4.62	2.91-4.35

† Tolerance based on $\pm$ 20% χ_f.

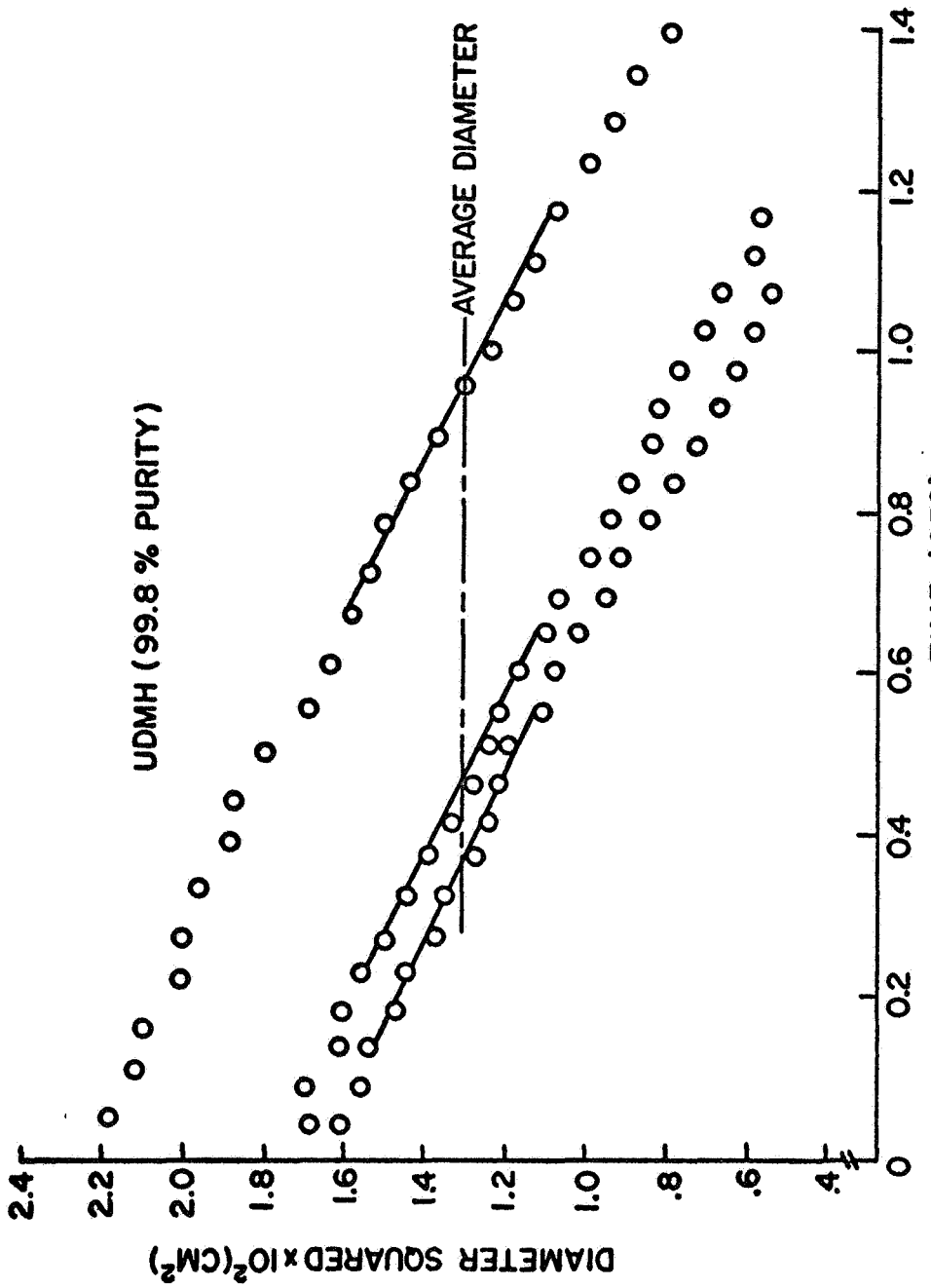

Fig. 1 Variation of droplet diameter squared as a function of time for UDMH at atmospheric pressure, 2470 K, $Y_x = 0$, $V = 55.7$ cm/sec.

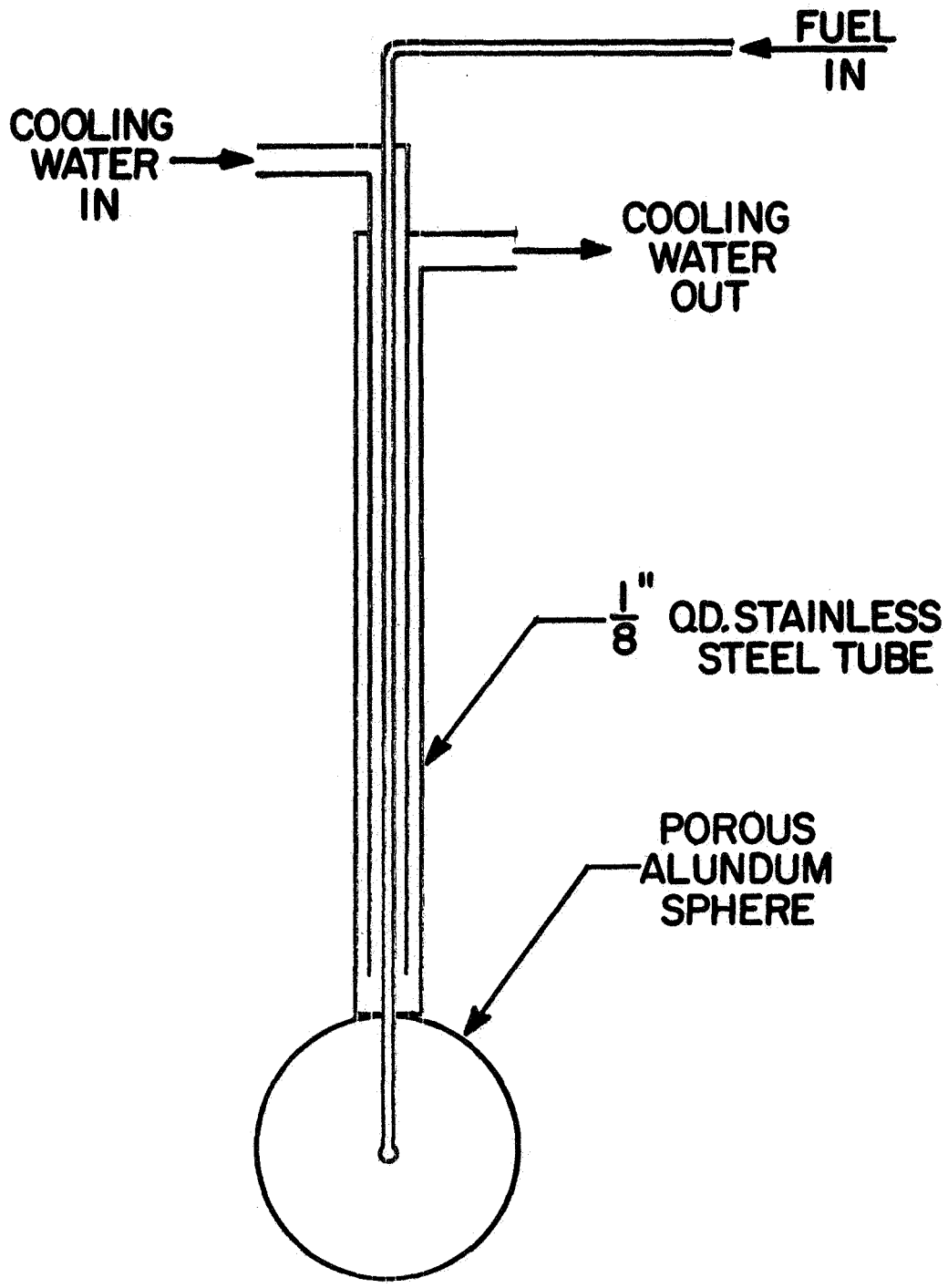

Fig. 2 Porous Sphere Probe.

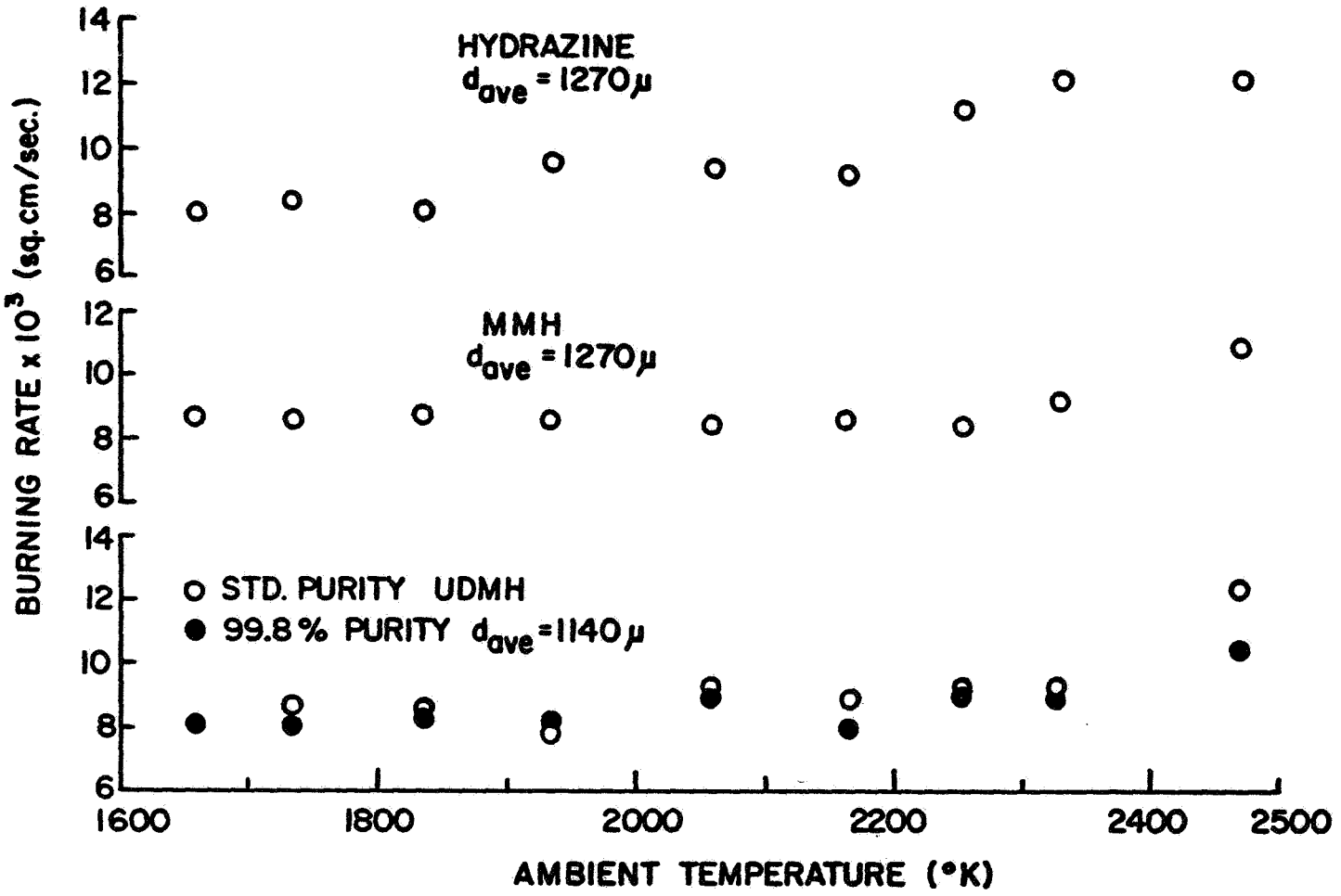

Fig. 3 Influence of ambient temperature on the burning rate of hydrazine, MMH and UDMH at atmospheric pressure, $Y_x = 0$, V = 55.7 cm/sec.

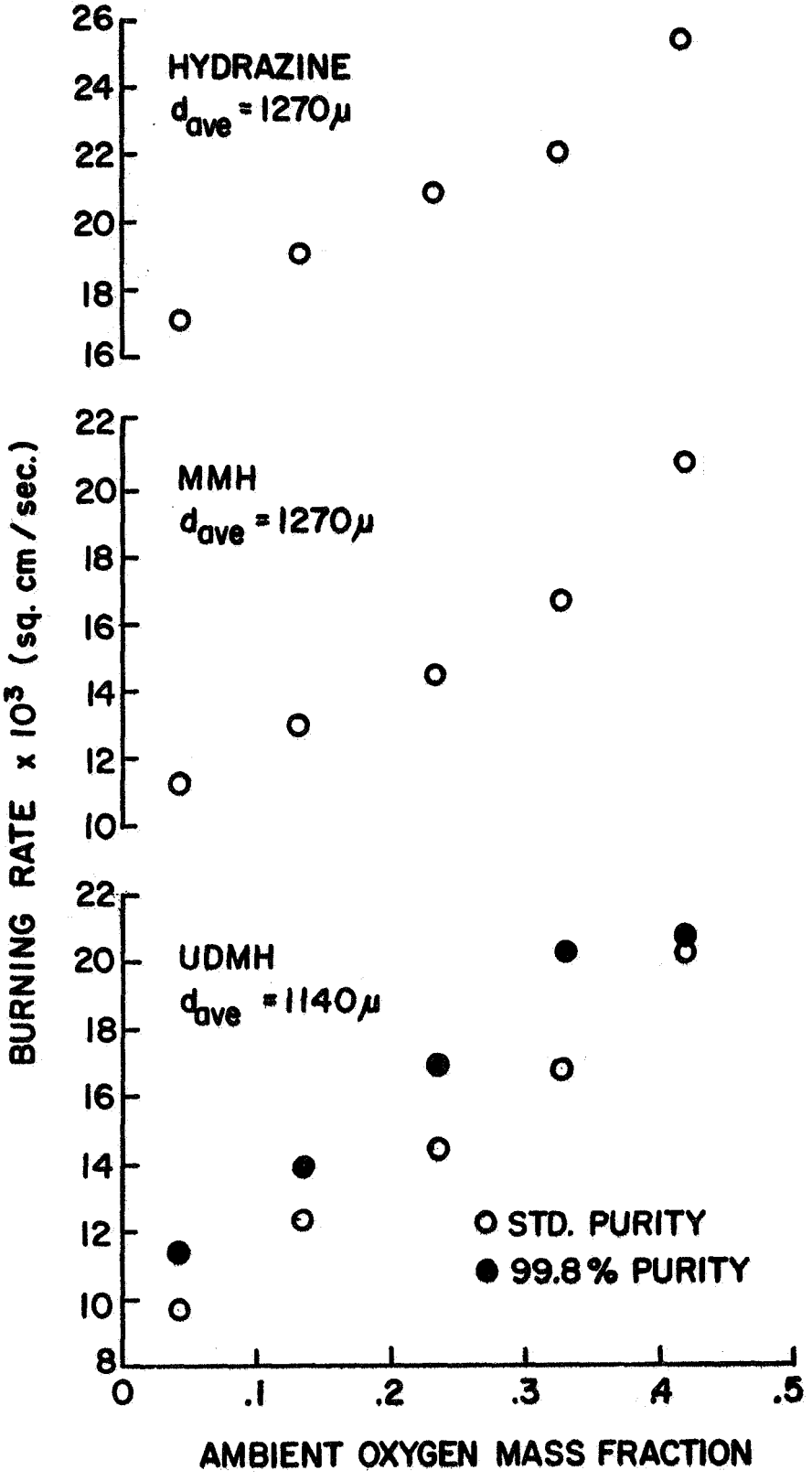

Fig. 4 Influence of ambient oxygen mass friction on the burning rate of hydrazine, MMH, and UDMH at atmospheric pressure, T = 2530 K, V = 53.4 cm/sec.

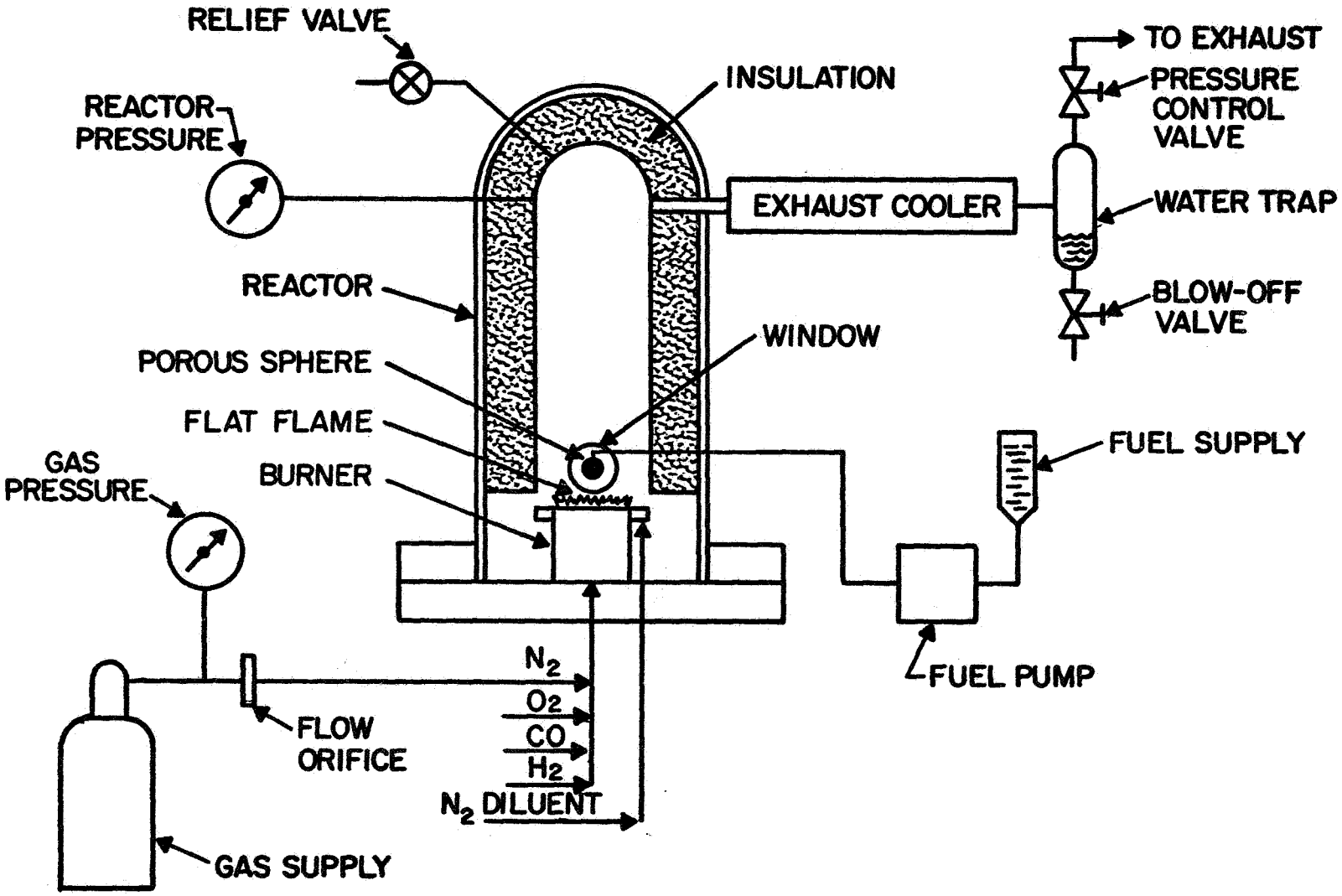

Fig. 5 Sketch of the high pressure flat flame burner apparatus.

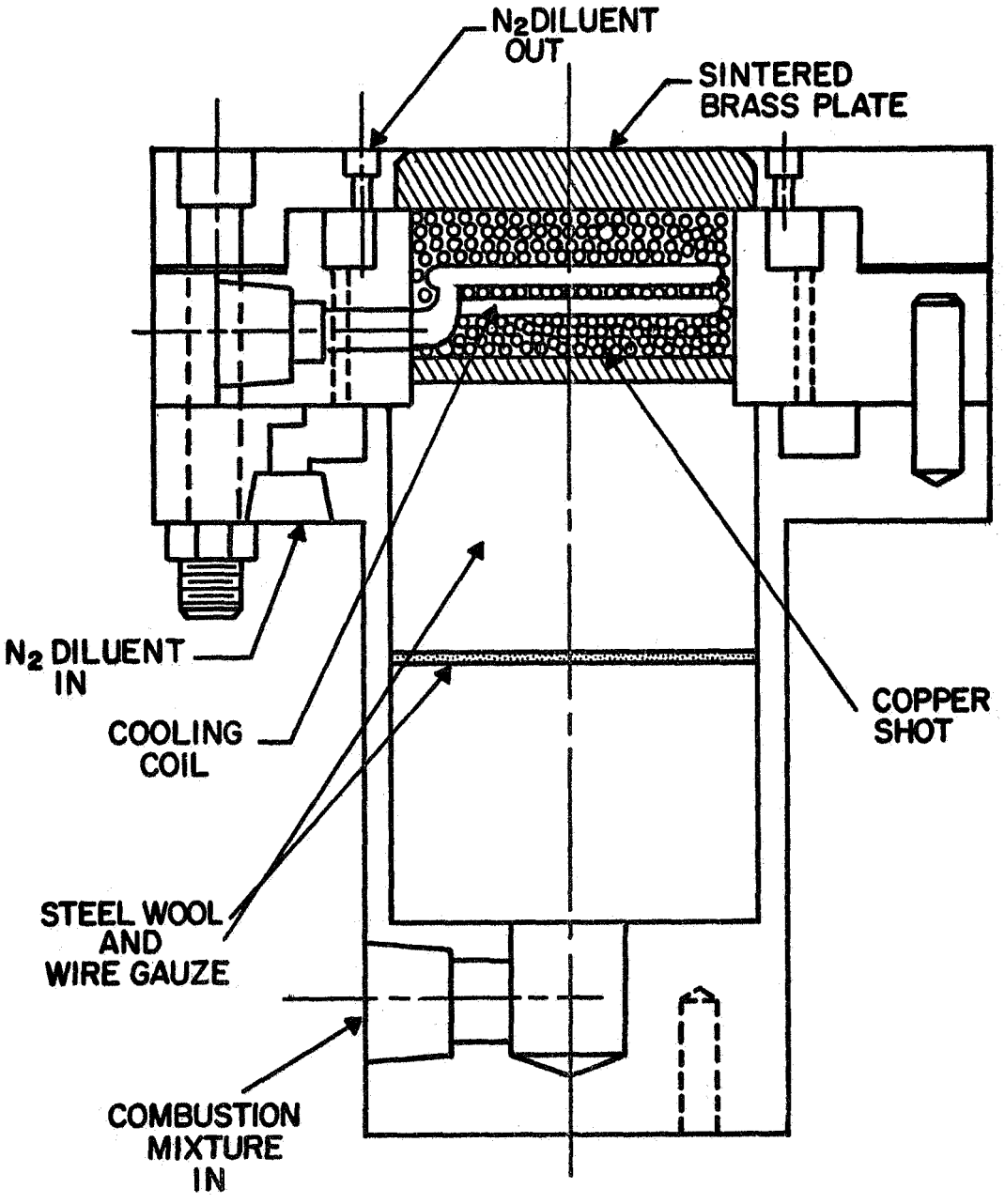

Fig. 6 High Pressure Flat Flame Burner.

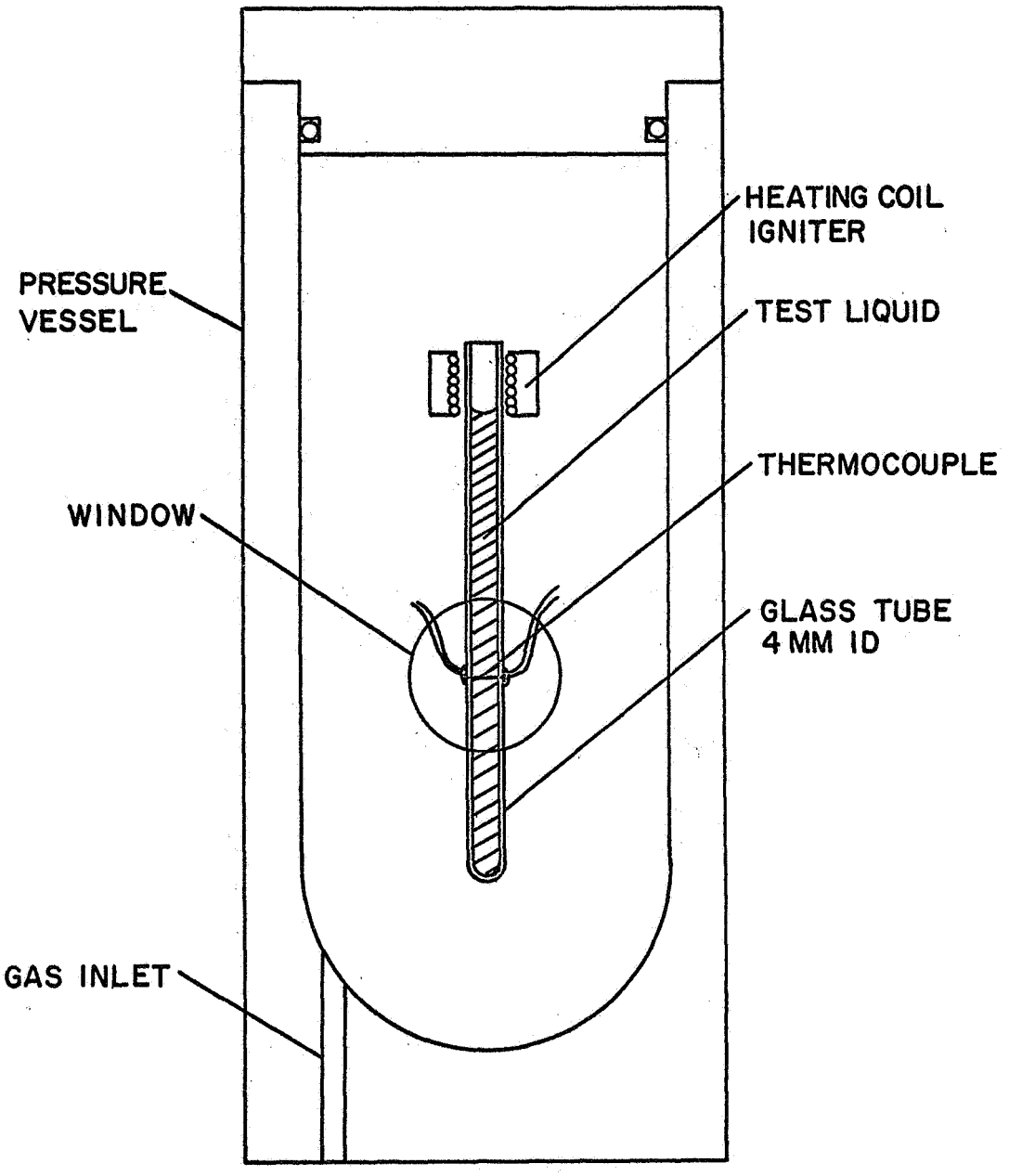

Fig. 7 Sketch of the Strand Burner Apparatus.

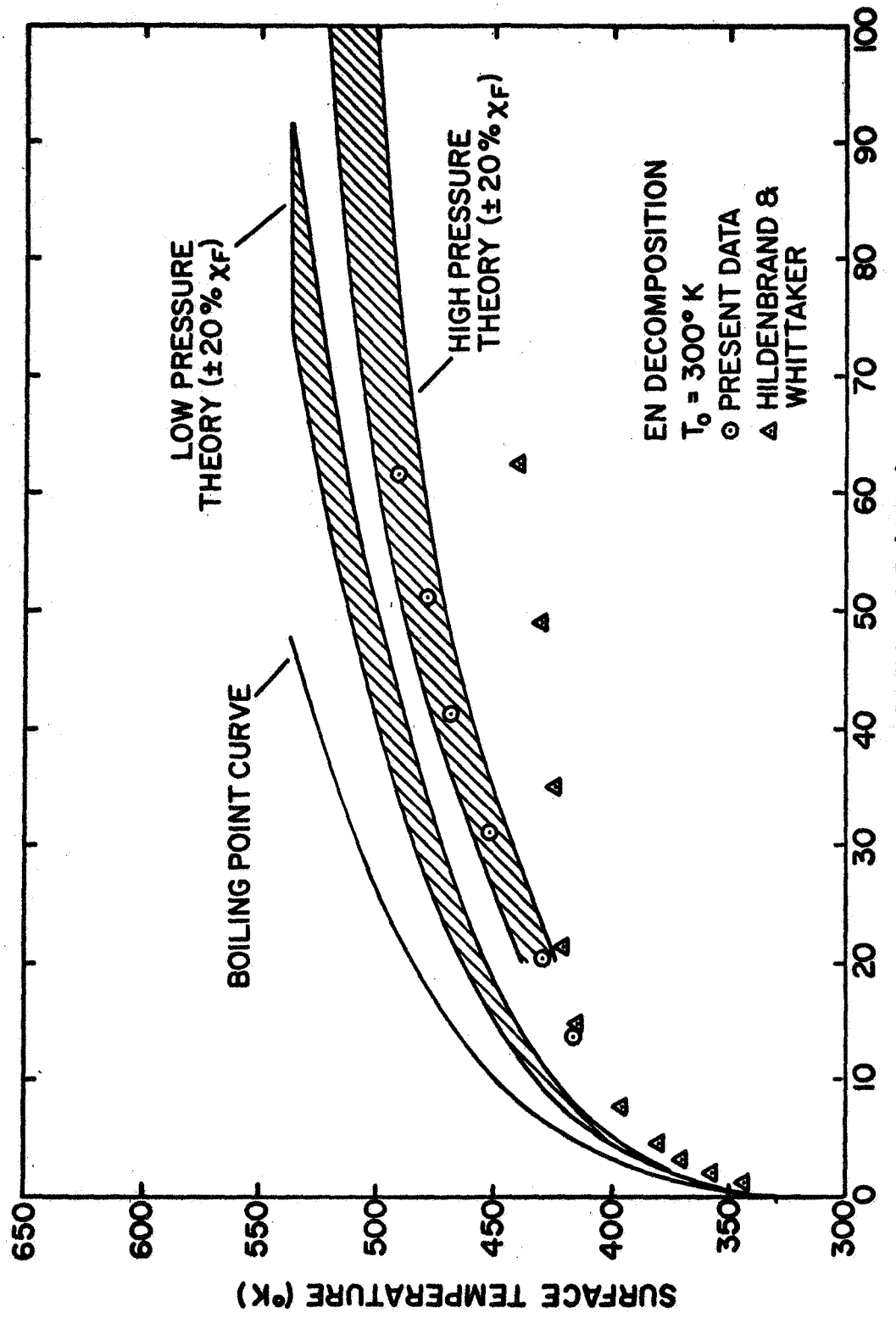

Fig. 8 EN surface temperatures as a function of pressure.

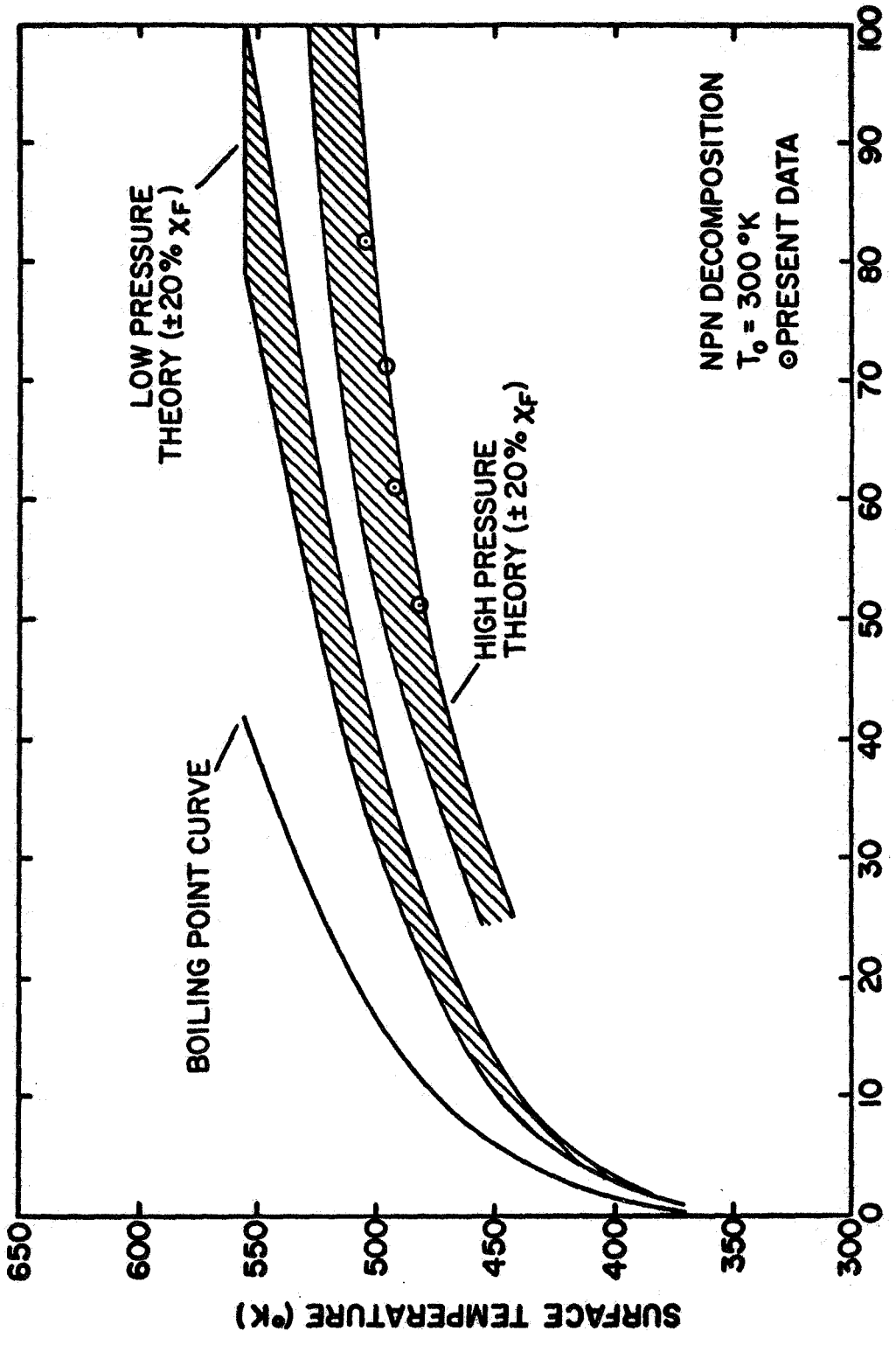

Fig. 9 NPN surface temperatures as a function of pressure.

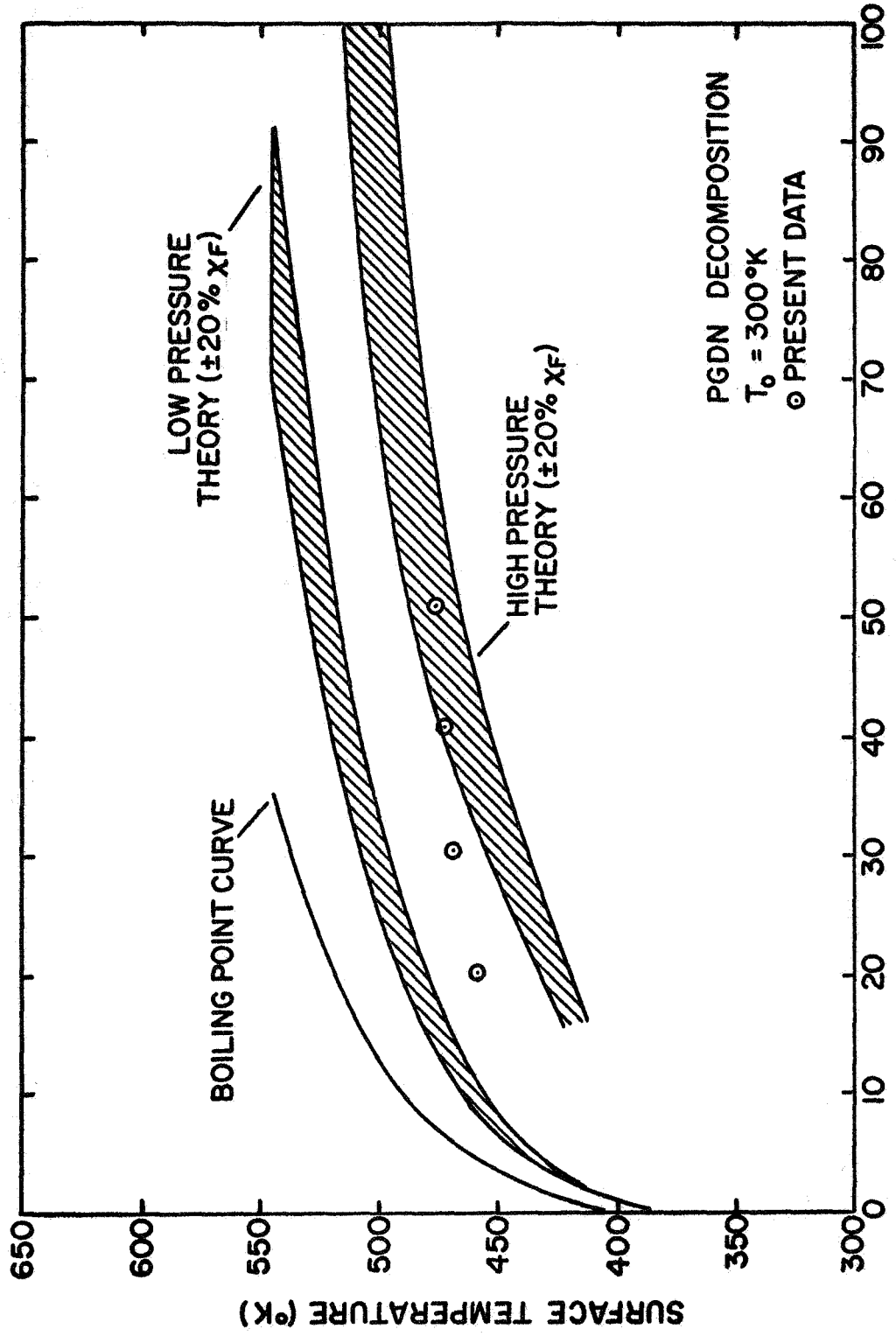

Fig. 10 PGDN surface temperatures as a function of pressure.

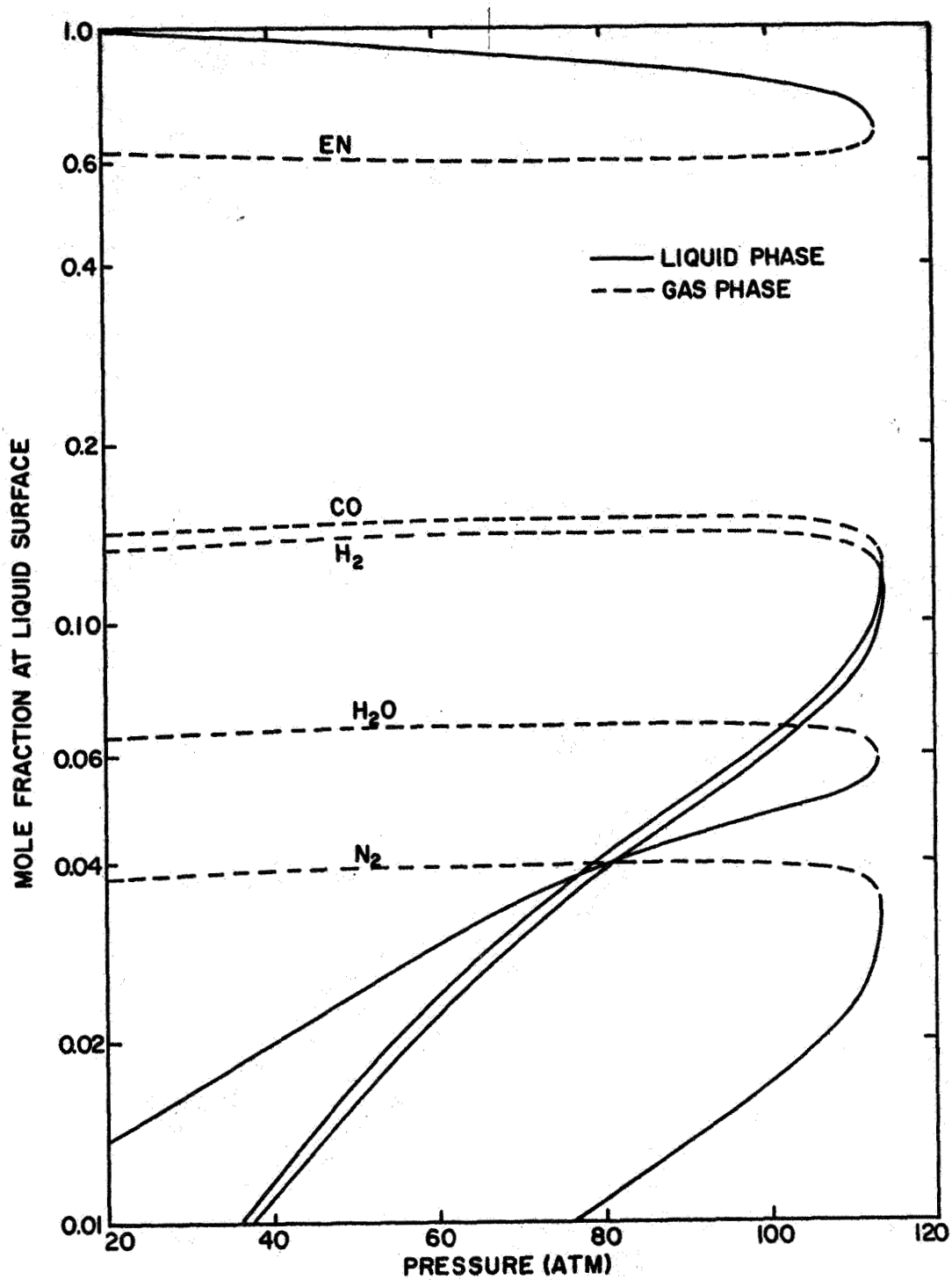

Fig. 11 Mole Fractions at the Liquid Surface for EN as a Function of Pressure.

REPORT DISTRIBUTION LIST OF

CONTRACT NO. NGR 39-009-077

Dr. R. J. Priem MS 500-204
NASA Lewis Research Center
21000 Brookpark Road
Cleveland, Ohio 44135 (2)

Norman T. Musial
NASA Lew Research Center
21000 Brookpark Road
Cleveland, Ohio 44135

Library (2)
NASA Lewis Research Center
21000 Brookpark Road
Cleveland, Ohio 44135

Report Control Office
NASA Lewis Research Center
21000 Brookpark Road
Cleveland, Ohio 44135

NASA Representative (6)
NASA Scientific and Technical
Information Facility
P.O. Box 33
College Park, Maryland 20740

V. Agosta
Brooklyn Polytechnic Institute
Long Island Graduate Center
Route 110
Farmingdale, New York 11735

L. Zung
Dynamic Science, a Division of
Marshall Industries
1900 Walker Avenue
Monrovia, California 91016

Thomas J. Chew
AFRPL (RPPZ)
Edwards, California 93523

T. W. Christian
Chemical Propulsion Information Agency
8621 Georgia Avenue
Silver Spring, Maryland 20910

R. M. Clayton
Jet Propulsion Laboratory
California Institute of Technology
4800 Oak Grove Drive
Pasadena, California 91103

E. W. Conrad MS 500-204
NASA Lewis Research Center
21000 Brookpark Road
Cleveland, Ohio 44135

Dr. E. K. Dabora
University of Connecticut
Aerospace Department
Storrs, Connecticut 06268

O. W. Dykema
Aerospace Corporation
P.O. Box 95085
Los Angeles, California 90045

G. W. Elverum
TRW Systems
1 Space Park
Redondo Beach, California 90278

R. Edse
Ohio State University
Dept. of Aeronautical and
Astronautical Engineering
Columbus, Ohio 43210

G. D. Garrison
Pratt and Whitney Aircraft
Florida Research And Development Ctr.
P. O. Box 2691
West Palm Beach, Florida 33402

M. Gerstein
Dept. Mechanical Engineering
University of Southern California
University Park
Los Angeles, California 90007

I. Glassman
Princeton University
James Forrestal Research Center
P.O. Box 710
Princeton, New Jersey 08540

Richard W. Haffner
Air Force Office of Scientific Research
1400 Wilson Blvd.
Arlington, Virginia 22209

D. Harrje
Princeton University
James Forrestal Research Center
P.O. Box 710
Princeton, New Jersey 08540

T. Inouye Code 4581
U. S. Naval Weapons Center
China Lake, California 93555

R. D. Jackel, 429
Office of Naval Research
Navy Department
Washington, D. C. 20360

T. Coultas
Rocketdyne
A Division of North American Aviation
6633 Canoga Avenue
Canoga Park, California 91304

R. S. Levine, Code RPL
NASA Headquarters
6th and Independence Ave., S.W.
Washington, D. C. 20546

Don Nored MS 500-209
NASA Lewis Research Center
21000 Brookpark Road
Cleveland, Ohio 44135

J. M. McBride
Aerojet-General Corporation
P.O. Box 15847
Sacramento, California 95809

P. D. McCormack
Dartmouth University
Hanover, New Hampshire 03755

C. E. Mitchell
Colorado State University
Fort Collins, Colorado 80521

P. S. Myers
University of Wisconsin
Mechanical Engineering Dept.
1513 University Avenue
Madison, Wisconsin 53705

J. A. Nestlerode
Rocketdyne
A Division of North American Aviation
6633 Canoga Avenue
Canoga Park, California 91304

J. A. Nicholls
University of Michigan
Aerospace Engineering
Ann Arbor, Michigan 48104

James C. O'Hara
Tulane University
Dept. of Mechanical Engineering
New Orleans, La. 70118

A. K. Oppenheim
University of California
Dept. of Aeronautical Sciences
6161 Etcheverry Hall
Berkeley, California 94720

Dr. K. Ragland
University of Wisconsin
Mechanical Engineering Dept.
Madison, Wisconsin 53705

Dr. A. A. Ranger
Purdue University
School of Aeronautics, Astronautics, and Engineering Sciences
Lafayette, Indiana 47907

F. H. Reardon
Sacramento State College
School of Engineering
6000 J. Street
Sacramento, California 95819

B. A. Reese
Purdue University
School of Mechanical Engr.
Lafayette, Indiana 47907

R. J. Richmond, S&E-ASTN-PP-70-L-7
NASA George C. Marshall Space
Flight Center
Huntsville, Alabama 35812

J. H. Rupe
Jet Propulsion Laboratory
California Institute of Technology
4800 Oak Grove Drive
Pasadena, California 91103

Dr. R. F. Sawyer
University of California
Mechanical Engineering, Thermal Systems
Berkeley, California 94720

K. Scheller
ARL (ARC)
Wright-Patterson AFB
Dayton, Ohio 45433

Roger A. Strehlow
University of Illinois
Aeronautical Engineering Dept.
Urbana, Illinois 61801

J. G. Thibadaux
NASA Manned Spacecraft Center
Houston, Texas 77058

T. P. Torda
Illinois Institute of Technology
Room 200 M.H.
3300 S. Federal Street
Chicago, Illinois 60616

T. Y. Toong
Massachusetts Institute of Technology
Department of Mechanical Engineering
Cambridge, Massachusetts 02139

Richard Weiss
AFRPL
Edwards, California 93523

W. W. Wharton AMSMI-RKL
U. S. Army Missile Command
Redstone Arsenal, Alabama 35808

F. A. Williams
University of California
Aerospace Engineering Dept.
P.O. Box 109
LaJolla, California 92038

L. M. Wood
Bell Aerosystems Company
P.O. Box 1
Mail Zone J-81
Buffalo, New York 14205

B. T. Zinn
Georgia Institute of Technology
Aerospace School
Atlanta, Georgia 30332

Library
Goddard Space Flight Center
(NASA)
Greenbelt, Maryland 20771

Library
NASA John F. Kennedy Space Ctr.
Cocoa Beach, Florida 32931

Library
NASA Langley Research Center
Langley Station
Hampton, Virginia 23365

Library
NASA Manned Spacecraft Center
Houston, Texas 77001

Library
NASA George C. Marshall Space
Flight Center
Huntsville, Alabama 35812

Library
Jet Propulsion Laboratory
4800 Oak Grove Drive
Pasadena, California 91103

Library
NASA Flight Research Center
P. O. Box 273
Edwards, California 93523

Library
NASA Ames Research Center
Moffett Field, California 94035

TISIA
Defense Documentation Center
Cameron Station
Building 5
5010 Duke Street
Alexandria, Virginia 22314

Office of Asst. Dire. (Chem. Techn.)
Office of the Director of Defense
Research & Engineering
Washington, D. C. 20301

D. E. Mock
Advanced Research Projects Agency
Washington, D. C. 20525

Dr. H. K. Doetsch
Arnold Engineering Development Center
Air Force Systems Command
Tullahoma, Tennessee 37389

Library
Air Force Rocket Propulsion Laboratory
(RPR)
Edwards, California 93523

Library
Bureau of Naval Weapons
Department of the Navy
Washington, D. C.

Library
Director (Code 6180)
U. S. Naval Research Laboratory
Washington, D. C. 20390

APRP (Library
Air Force Aero Propulsion Laboratory
Research & Technology Division
Air Force Systems Command
United States Air Force
Wright-Patterson AFB, Ohio 45433

Technical Information Department
Aeronutronic Division of Philco Ford Corp.
Ford Road
Newport Beach, California 92663

Library-Documents
Aerospace Corporation
2400 E. El Segundo Blvd.
Los Angeles, California 90045

Library
Bell Aerosystems, Inc.
Box 1
Buffalo, New York 14205

Report Library, Room 6A
Battelle Memorial Institute
505 King Avenue
Columbus, Ohio 43201

D. Suichu
General Electric Company
Flight Propulsion Lab. Dept.
Cincinnati, Ohio 45215

Library
Ling-Temco-Vought Corp.
P. O. Box 5907
Dallas, Texas 75222

Marquardt Corporation
16555 Saticoy Street
Box 2013 - South Annex
Van Nuys, California 91409

P. F. Winternitz
New York University
University Heights
New York, New York

I. Forsten
Picatinny Arsenal
Dover, New Jersey 07801

R. Stiff
Propulsion Division
Aerojet-General Corporation
P. O. Box 15847
Sacramento, California 95803

Library, Department 596-306
Rocketdyne Division of Rock-
well
North American Rockwell Inc.
6633 Canoga Avenue
Canoga Park, California 91304

Library
Stanford Research Institute
333 Ravenswood Avenue
Menlo Park, California 94025

Library
Susquehanna Corporation
Atlantic Research Division
Shirley Highway & Edsall Road
Alexandria, Virginia 22314

STL Tech. Lib. Doc. Acquisitions
TRW System Group
1 Space Park
Redondo Beach, California 90278

Dr. David Altman
United Aircraft Corporation
United Technology Center
P. O. Box 358
Sunnyvale, California 94088

Library
United Aircraft Corporation
Pratt & Whitney Division
Florida Research & Development Center
P. O. Box 2691
West Palm Beach, Florida 33402

Library
Air Force Rocket Propulsion Laboratory (RPM)
Edwards, California 93523